Geophysical Research Letters

RESEARCH LETTER
10.1029/2020GL088292

Key Points:
- A predictive model for tracer dispersion in highly heterogeneous aquifers is presented
- The model is parameterized by transport-independent parameters
- The large-scale evolution of the tracer profiles of the MADE-1 and MADE-2 experiments is predicted

Supporting Information:
- Supporting Information S1

Correspondence to:
M. Dentz,
marco.dentz@csic.es

Citation:
Dentz, M., Comolli, A., Hakoun, V., & Hidalgo, J. J. (2020). Transport upscaling in highly heterogeneous aquifers and the prediction of tracer dispersion at the MADE site. *Geophysical Research Letters*, *47*, e2020GL088292. https://doi.org/10.1029/2020GL088292

Received 8 APR 2020
Accepted 25 OCT 2020

©2020. American Geophysical Union. All Rights Reserved.

Transport Upscaling in Highly Heterogeneous Aquifers and the Prediction of Tracer Dispersion at the MADE Site

Marco Dentz[1], Alessandro Comolli[1,2], Vivien Hakoun[1,3], and Juan J. Hidalgo[1]

[1]Spanish National Research Council (IDAEA-CSIC), Barcelona, Spain, [2]Nonlinear Physical Chemistry Unit, Université Libre de Bruxelles (ULB), Brussels, Belgium, [3]BRGM, University of Montpellier, Montpellier, France

Abstract We present an upscaled Lagrangian approach to predict the plume evolution in highly heterogeneous aquifers. The model is parameterized by transport-independent characteristics such as the statistics of hydraulic conductivity and the Eulerian flow speed. It can be conditioned on the tracer properties and flow data at the injection region. Thus, the model is transferable to different solutes and hydraulic conditions. It captures the large-scale non-Gaussian features for the evolution of the longitudinal mass distribution observed for the bromide and tritium tracer plumes at the Macrodispersion Experiment (MADE) site (Columbus, Mississippi, USA), which are characterized by a slow moving peak and pronounced forward tailing. These large-scale features are explained by advective tracer propagation due to a broad distribution of spatially persistent Eulerian flow speeds as a result of spatial variability in hydraulic conductivity.

Plain Language Summary The prediction of solute transport in highly heterogeneous porous media has been a long-standing question. We propose an approach that predicts and explains observed tracer distributions in terms of medium and flow heterogeneity. The model is parameterized by the statistical characteristics of hydraulic conductivity, distribution of flow speeds, porosity, and retardation coefficient, that is, transport-independent parameters. This study gives new insight for the understanding and prediction of large-scale tracer dispersion in heterogeneous aquifers.

1. Introduction

The upscaling and prediction of tracer transport in highly heterogeneous porous and fractured media are of central concern in a broad range of subsurface applications from groundwater management to underground gas and waste storage. This task is challenging due to strong spatial variability in hydraulic conductivity values encountered in geological media (Bear, 1972).

Spatial variability in hydraulic conductivity induces spatial fluctuations in the flow and transport velocities, whose impact on large-scale tracer migration has been quantified in terms of macrodispersion coefficients (Dagan, 1984; Gelhar & Axness, 1983). For moderately heterogeneous media, Gelhar and Axness (1983) used a stochastic modeling approach (Dagan, 1989; Gelhar, 1993; Rubin, 2003) to express the longitudinal macrodispersion coefficients in terms of the mean flow velocity and the correlation length and variance of the logarithm of hydraulic conductivity. This expression is a central result for hydrogeological prediction because it allows forecasting macroscopic transport features based on transport-independent observables.

However, spatial heterogeneity gives rise to transport behaviors that can be very different from the ones predicted by advection-dispersion models characterized by constant macrodispersion coefficients. For pointlike solute injections, the latter predicts Gaussian-shaped tracer plumes and breakthrough curves, while observed distributions are typically found to be non-Gaussian (Adams & Gelhar, 1992; Haggerty et al., 2000; Kang et al., 2015; Levy & Berkowitz, 2003; Zheng et al., 2011). This is the case for the tracer plumes monitored during the macrodispersion experiments conducted in the alluvial aquifer underlying the Columbus Air Force Base in northeastern Mississippi (Adams & Gelhar, 1992; Boggs et al., 1992). Spatial tracer distributions show strongly non-Gaussian shapes characterized by a slowly moving peak and a pronounced forward tail. These and other observations of anomalous solute dispersion have spurred the development of non-Fickian transport theories (Berkowitz et al., 2006; Dentz et al., 2011; Neuman & Tartakovsky, 2008; Noetinger et al., 2016). Those include multirate mass transfer (MRMT) approaches (Carrera et al., 1998;

Haggerty & Gorelick, 1995), continuous time random walks (CTRWs) (Berkowitz & Scher, 1997; Berkowitz et al., 2006), fractional advection-dispersion models (Benson et al., 2000; Cushman & Ginn, 2000), time-domain random walks (TDRWs) (Cvetkovic et al., 1996; Fiori et al., 2007), and space-time nonlocal advection-dispersion equations (Cushman & Ginn, 1993; Neuman, 1993). While all of these approaches provide dynamic frameworks to model non-Gaussian large-scale transport features, their parameterization in terms of transport-independent parameters and thus their predictive power remain open questions.

The migration of the tracer plume at the Macrodispersion Experiment (MADE) site was modeled by Berkowitz and Scher (1998) with the CTRW approach based on an empirical distribution of transition length and times, which reflects a broad distribution of mass transfer time scales. Benson et al. (2001), Schumer et al. (2003), and Zhang and Benson (2008) modeled the tracer plumes of the MADE-1 experiment using a fractal mobile-immobile model that accounts for both solute retention due to a broad distribution of mass transfer time scales and preferential transport due to a broad distribution of mass transfer length scales. The characteristic exponents of the model are estimated from the experimental data. Harvey and Gorelick (2000) modeled the plume evolution using an MRMT model that considers rate-limited mass transfer between a mobile domain with accelerating flow and an immobile zone, which represents intragranular porosity, low permeability zones, dead end pores, and surface sorption sites. These different processes are represented by a capacity coefficient, a rate coefficient, a retardation coefficient, a velocity parameter, and an acceleration parameter, which are estimated from the experimental mass data. These modeling approaches propose a range of mass transfer processes and invoke broad distributions of mass transfer time scales and lengths in order to simulate the impact of medium and flow heterogeneity on large-scale transport. A key question in order to constrain such models refers to the dominant local scale mechanisms that cause non-Fickian large-scale transport.

Mobile-immobile mass transfer has been studied as a mechanism to explain the decay of the apparent solute mass observed at the MADE-1 and MADE-2 experiments (Harvey & Gorelick, 2000). Feehley et al. (2000) and Guan et al. (2008) combine a stochastic reconstruction of aquifer heterogeneity based on fractal Brownian motion with mobile-immobile mass transfer in order to assess the plume evolution in the MADE-2 experiment. A series of works (Barlebo et al., 2004; Dogan et al., 2016; Salamon et al., 2007) have shown that a local-scale advection-dispersion model based on the detailed knowledge of the spatial distribution of hydraulic conductivity allows reproducing the spatial distribution of tracer plumes observed at the MADE site. This implies that some key features of transport may indeed be understood from the spatial variability of hydraulic conductivity and thus advective heterogeneity. The question arising from this observation is whether characteristics of non-Fickian transport in strongly heterogeneous media can be predicted based only on a few geostatistical medium characteristics similar to the prediction of macrodispersion in moderately heterogeneous media. Along these lines, several authors (Cvetkovic et al., 2014; Edery et al., 2014; Fiori et al., 2007; Tyukhova et al., 2016) investigated the relation between advective travel times and hydraulic conductivity and the impact of broad distributions of the logarithm of hydraulic conductivity on non-Fickian transport. For example, the stochastic multi-indicator approach of Fiori et al. (2007) was adapted in Fiori et al. (2013) to predict the plume evolution of the MADE-1 experiment based on analytical expressions for the advective travel times over rectangular inclusions.

In this paper, we address the questions of upscaling and prediction of dispersion in highly heterogeneous aquifers in terms of medium and flow heterogeneity using transport-independent parameters. We use a stochastic TDRW approach (Comolli et al., 2019; Hakoun et al., 2019) that accounts for heterogeneous advection. This approach propagates particles in space and time according to a velocity Markov model that is determined by the distribution of the Eulerian flow speed and correlation length. We discuss the model and its parameterization in terms of the medium and flow properties and use it for the modeling and interpretation of the one-dimensional tracer profiles of the MADE-1 experiment.

2. Upscaled Transport Model

We employ the stochastic TDRW implementation presented in Comolli et al. (2019) in order to build an upscaled model to predict the concentration evolution in highly heterogeneous aquifers, based on the statistical characteristics of the logarithm of hydraulic conductivity, the flow speed, porosity, and the mean hydraulic gradient. The method quantifies particle motion in spatially variable flow fields through a

stochastic model for equidistantly sampled particle speeds along streamlines. Thus, it propagates solute particles at constant space increments whose duration is obtained from a Markov chain representation for the particle speed. The model is predictive because it can be parameterized by transport-independent medium and flow characteristics. This approach has been used for the upscaling and prediction of solute transport from the pore to Darcy scale and from the Darcy to the field scale in two- and three-dimensional porous and fractured media (Comolli et al., 2019; Hyman et al., 2019; Kang et al., 2011, 2014, 2015, 2017; Le Borgne et al., 2008; Morales et al., 2017; Puyguiraud et al., 2019a). In the following, we detail the model, its assumptions, and parameterization.

We choose a Lagrangian framework (Dagan, 1989) and focus on the advective motion of tracer particles, which constitute the tracer plume. The temporal variation patterns of particle velocities are in general rather complex. They are intermittent because their evolution is governed by a broad distribution of times scales, which are determined by the flow speeds and characteristic length scales imprinted in the medium structure (Dentz et al., 2016; Hakoun et al., 2019). The complexity of intermittent temporal series of particle velocities can be removed by adopting an equidistant point of view. Therefore, unlike classical Lagrangian approaches, we do not consider particle motion isochronally but equidistantly along streamlines. This means we quantify motion through transitions over constant space increments instead of constant time increments. It has been shown for the pore and the Darcy scale (Hakoun et al., 2019; Hyman et al., 2019; Le Borgne et al., 2008; Puyguiraud et al., 2019b) that equidistant series of particle velocities can be modeled as Markov chains.

Thus, advective particle motion is quantified by the following stochastic evolution equations for the longitudinal particle position $x(s)$ and the advective travel time $t_a(s)$ (Dentz et al., 2016; Comolli et al., 2019):

$$\frac{dx(s)}{ds} = \chi^{-1}, \quad \frac{dt_a(s)}{ds} = \frac{1}{v_\ell(s)}, \tag{1}$$

where s is the distance along streamline and $v_\ell(s) > 0$ the particle speed, meaning the magnitude of the equidistant particle velocity. The distance s along the streamline is in general larger than the linear travel distance x in the mean flow direction. They are projected onto each other through the advective tortuosity χ, which is given by the ratio of the average flow speed $\langle q \rangle$ and the average velocity component $\langle q_1 \rangle$ in mean flow direction, $\chi = \langle q \rangle / \langle q_1 \rangle$ (Comolli et al., 2019). The angular brackets denote suitably chosen averages, here spatial and ensemble average. The particle speed $v_\ell(s)$ describes an ergodic and stationary Markov process characterized by the steady-state distribution $p_v(v)$. The latter is a Lagrangian quantity, which, however, can be related to the distribution of Eulerian flow speed $p_e(v)$ via the flux-weighting relation (Dentz et al., 2016; Comolli et al., 2019):

$$p_v(v) = \frac{v p_e(v)}{\langle v \rangle}. \tag{2}$$

Note that $v_\ell(s)$ evolves as a function of distance s along a streamline, while in classical Lagrangian methods (Dagan, 1989), particle speeds evolve with travel time. This difference explains the flux-weighting relationship (2) as discussed in detail in Dentz et al. (2016) and Hakoun et al. (2019).

The Eulerian velocity $\mathbf{v}(\mathbf{x})$ is given in terms of the Darcy flux $\mathbf{q}(\mathbf{x})$, porosity ϕ, and the retardation coefficient θ, which accounts for linear equilibrium sorption. We assume that both porosity and retardation are constant. The Darcy flux satisfies

$$\mathbf{q}(\mathbf{x}) = -K(\mathbf{x}) \nabla h(\mathbf{x}), \quad \nabla \cdot \mathbf{q}(\mathbf{x}) = 0, \tag{3}$$

where $K(\mathbf{x})$ is hydraulic conductivity and $h(\mathbf{x})$ hydraulic head. The flow problem (3) is solved numerically for a unit mean hydraulic gradient aligned with the coordinate axis in one direction and a unit geometric mean conductivity $K_g = 1$; see section S2 in the supporting information. The Eulerian velocity $\mathbf{v}(\mathbf{x})$ is given in terms of the resulting Darcy velocity $\mathbf{q}(\mathbf{x})$ as

$$\mathbf{v}(\mathbf{x}) = v_0 \mathbf{q}(\mathbf{x}), \quad v_0 = K_g J / \phi\theta, \tag{4}$$

where J is the magnitude of the mean hydraulic gradient. The velocity v_0 and the correlation length ℓ_c

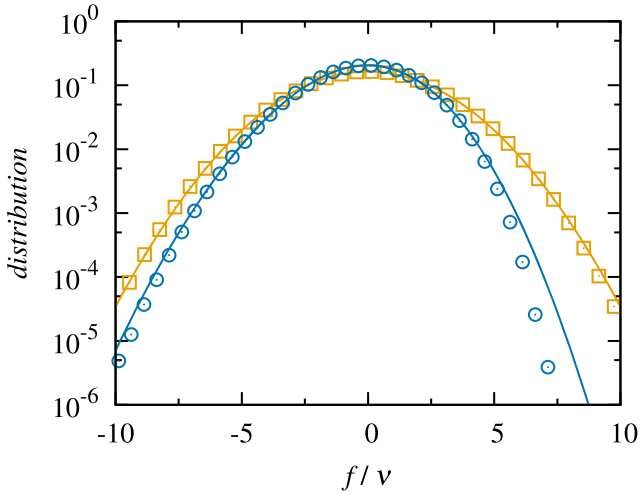

Figure 1. Empirical distribution of $f(\mathbf{x})$ (squares). The solid orange line denotes the normal distribution with zero mean and variance $\sigma_f^2 = 5.9$. Empirical distribution of the logarithm $\nu(\mathbf{x})$ of the flow speed (circles). The blue solid line denotes the skewed normal distribution (6).

define the characteristic time $\tau_v = \ell_c/v_0$. Note that changes in v_0 affect transport only through a rescaling of time. The Eulerian speed is $v(\mathbf{x}) = |\mathbf{v}(\mathbf{x})|$, and its distribution is, as introduced above, denoted by $p_e(v)$. The magnitude of $\mathbf{q}(\mathbf{x})$ is denoted by $q(\mathbf{x})$. Based on (4), the Eulerian speed distribution is given in terms of the distribution $p_q(q)$ of $q(\mathbf{x})$ as

$$p_e(v) = p_q(v/v_0)/v_0. \tag{5}$$

In this work, hydraulic conductivity is represented by a three-dimensional lognormally distributed spatial random field. The horizontal correlation length is $\ell_h = 5\ell_v$, and the variance of the logarithm $f(\mathbf{x}) = \ln[K(\mathbf{x})]$ of hydraulic conductivity is set to $\sigma_f^2 = 5.9$ reflecting the conductivity statistics estimated for the MADE site (Bohling et al., 2016). We find $\langle q_1 \rangle = 3.04$ and $\langle q \rangle = 3.5$. This implies that the effective conductivity is $K_e = 3.04K_g$ and the advective tortuosity $\chi = 1.15$. Figure 1 shows the distributions of $f(\mathbf{x}) = \ln[K(\mathbf{x})]$ and $\nu(\mathbf{x}) = \ln[q(\mathbf{x})]$. The distribution $p_\nu(\nu)$ of $\nu(\mathbf{x})$ can be modeled by the skewed Gaussian distribution

$$p_\nu(\nu) = \frac{\exp\left[-\dfrac{(\nu - m)^2}{2\sigma_\nu^2}\right]}{\sqrt{2\pi\sigma_\nu^2}} \Phi\left[\alpha(\nu - m)/\sqrt{\sigma_\nu^2}\right], \tag{6}$$

where $\Phi(x)$ is the cumulative unit Gaussian distribution. The parameters in Figure 1 are $\sigma_\nu^2 = \sigma_f^2 = 5.9$, $\alpha = 1.29$, and $m = 1.47$.

Regarding the propagation of the particle speeds $v_\ell(s)$ from their initial values $v_0 = v_\ell(0)$, the key feature is the spatial persistence of speeds, which is characteristic for transport in steady flow fields (Berkowitz & Scher, 1997; Cvetkovic et al., 1996; Dentz et al., 2016; Le Borgne et al., 2008). This spatial persistence is at the origin of intermittent Lagrangian flow properties in porous media found both at the pore and Darcy scales (de Anna et al., 2013; Hakoun et al., 2019; Morales et al., 2017; Puyguiraud et al., 2019b). Thus, velocity transitions have been modeled, for example, through independent sampling after fixed persistence lengths (Berkowitz et al., 2006), Bernoulli processes (Dentz et al., 2016; Hakoun et al., 2019; Kang et al., 2015), and by empirical velocity transition matrices (Le Borgne et al., 2008; Kang et al., 2011). In this work, we consider the evolution of the normal score $w(s)$ of $v_\ell(s)$, which is given by

$$w = \Phi^{-1}[P_v(v)], \quad v = P_v^{-1}[\Phi(w)]. \tag{7}$$

The cumulative probability of $p_v(v)$ is denoted by $P_v(v)$, its inverse by $P_v^{-1}(v)$. The Doob theorem states that the only process that is both Markovian and Gaussian is the Ornstein-Uhlenbeck process (Doob, 1942; Gardiner, 1986). For this reason, we model the evolution of $w(s)$ through the Ornstein-Uhlenbeck process (Gardiner, 1986):

$$\frac{dw(s)}{ds} = -\ell_c^{-1} w(s) + \sqrt{2\ell_c^{-1}}\eta(s), \tag{8}$$

where $\eta(s)$ is a Gaussian white noise characterized by 0 mean and correlation $\langle \eta(s)\eta(s') \rangle = \delta(s - s')$. The steady-state distribution of $w(s)$ is the unit Gaussian. The initial values $w(0)$ of the normal scores are obtained from $v(0)$ through the Smirnov transform (7). The initial velocity distribution is denoted by $p_0(v)$. The correlation length ℓ_c of the normal score $w(s)$ is set equal to $\ell_c = 8\ell_h/3$ (Comolli et al., 2019; Cvetkovic et al., 1996; Hakoun et al., 2019). This approach has been used and verified for the prediction of equidistant Lagrangian velocity series and intermittent transport characteristics in pore and Darcy scale heterogeneous porous media (Comolli et al., 2019; Hakoun et al., 2019; Morales et al., 2017; Puyguiraud et al., 2019b).

Equations 1 together with the evolution equation for $v_\ell(s)$ describe the propagation of the particle position $x(s)$ and velocity $v_\ell(s)$ from the initial values $x(0)$ and $v(0)$, which are distributed according to $\rho(x)$ and $p_0(v)$. The initial value of time is $t(0) = 0$. The projected streamwise concentration profile $c(x, t)$ of the mobile, meaning nonadsorbed solute in this framework, is obtained by

$$c(x,\, t) = \theta^{-1}\langle \delta[x - s(t)/\chi]\rangle, \tag{9}$$

where $s(t) = \max[s|t_a(s) \le t]$. The angular brackets denote here the average over all particles. The TDRW approach is intrinsically mass conservative. Thus, its density describes the total, meaning the adsorbed and nonadsorbed concentrations, which is the reason why the nonadsorbed concentration is obtained from the total density through division by θ as given in Equation 9.

This stochastic TDRW approach is parameterized by the Eulerian speed distribution, advective tortuosity, and the correlation length ℓ_c. These quantities are constrained by the geometric mean conductivity, the variance, and correlation lengths of the logarithm of hydraulic conductivity, the mean hydraulic gradient, and porosity, without nonphysical fitting parameters. This means the model is parameterized in terms of geostatistical and hydraulic characteristics that can be determined by transport-independent measurements and is in this sense predictive. In addition, the approach can account for linear equilibrium sorption.

In the following, we use this upscaled transport model to predict the longitudinal plume evolution of the MADE-1 and MADE-2 experiments. Its numerical implementation is detailed in section S3.

3. Prediction of Dispersion at the MADE Site

We use the upscaled transport model presented in the previous section for the prediction of the streamwise tracer profiles of the MADE-1 and MADE-2 experiments (Adams & Gelhar, 1992; Boggs et al., 1993). For the MADE-1 experiment, we consider six snapshots of the longitudinal bromide concentration profiles (Adams & Gelhar, 1992; Fiori et al., 2013). For the MADE-2 experiment, we consider two snapshots of the longitudinal tritium profiles (Boggs et al., 1993; Salamon et al., 2007). In the following, we first discuss the model parameters for the MADE site and then report on the prediction of the longitudinal concentration profiles for the MADE-1 and MADE-2 experiments.

3.1. Hydraulic and Transport Parameters for the MADE Site

We consider purely advective transport, which is a reasonable assumption given that the Péclet number at the MADE site is around 10^3 (Fiori et al., 2013). In order to parameterize the model, we rely on the description of the experimental conditions in Boggs et al. (1992) and Adams and Gelhar (1992) and the geostatistical characterization of the hydraulic conductivity field given in Bohling et al. (2016). Thus, the medium porosity and the magnitude of the mean hydraulic gradient are set equal to $\phi = 0.31$, $J = 3.6 \times 10^{-3}$ (Adams & Gelhar, 1992; Boggs et al., 1992; Fiori et al., 2013). Bohling et al. (2016) estimate for the variance of the logarithm of conductivity $\sigma_f^2 = 5.9$ and for the horizontal and vertical correlation lengths $\ell_h = 9.1$ m and $\ell_v = 1.8$ m. For the geometric mean conductivity, these authors obtained the average value of $K_g = 6.7 \times 10^{-6}$ m/s. The upper and lower limits of the 95% confidence interval around this value are $K_g = 10^5$ m/s and $K_g = 4.3 \times 10^{-6}$ m/s. Here we use the value $K_g = 5.5 \times 10^{-6}$ m/s because it provides a better prediction of the observed peak concentration values than the average value. The model predictions for $K_g = 6.7 \times 10^{-6}$ m/s and a discussion of the evolution of the peak values are given in section S5.

The characteristic velocity v_0 is given by $v_0 = 6.39 \times 10^{-8}\theta^{-1}$ m/s and the average transport velocity by $\langle v_1\rangle = K_e J/\phi\theta = 1.94 \times 10^{-7}\theta^{-1}$ m/s. We use for the prediction of both the MADE-1 and MADE-2 data the same medium and hydraulic parameters. Boggs and Adams (1992) found from column experiments the values $\theta = 1.2$ and $\theta = 1$ for the retardation coefficients of bromide and tritium. The retardation coefficient accounts for the fact that only the mobile, nonadsorbed solute is measured (Boggs & Adams, 1992; Harvey & Gorelick, 2000) and in this sense accounts for a measurement bias.

The parameter values specified above determine the propagator of the upscaled transport model. In order to predict the plume evolution, we need both the propagator and the initial conditions, meaning the initial particle positions and initial particle speed distribution. As described in Boggs et al. (1992) and Stauffer

et al. (1994), in both experiments, tracer was injected in about 10 m^3 of groundwater for the duration of 48.5 hr into five 5.2-cm-diameter injection wells separated by 1 m in a linear array perpendicular to the mean flow direction. Thus, while the initial distribution of the tracer plume was indeed spatially extended in the transverse and longitudinal directions, we use here for simplicity a pointlike initial particle distribution, localized at the origin at $x = 0$:

$$\rho(x) = \delta(x). \tag{10}$$

Regarding the initial velocity distribution $p_0(v)$, we note that Boggs et al. (1992) and Fiori et al. (2013) pointed out that more mass entered in the high- than in the low-conductivity zones, which implies that the initial mass distribution is approximately flux-weighted. In order to set the initial velocity distribution $p_0(v)$, we assume that the initial plume extension is large enough to be considered ergodic (Fiori et al., 2013). Under this assumption, $p_0(v)$ can be set equal to $p_v(v)$ given by Equation 2. Note that the model can be conditioned on velocity data within the initial plume if detailed information is available. Below we use this approach to model and predict the longitudinal concentration profiles of the MADE-1 and MADE-2 experiments.

3.2. Longitudinal Concentration Profiles

The experimental concentration profiles for the MADE-1 experiment are based on the bromide tracer data from Adams and Gelhar (1992) normalized to the initial mass as given in Fiori et al. (2013). The concentration profiles for the tritium tracer at the MADE-2 experiment are obtained from Salamon et al. (2007).

Figures 2 and 3 show the experimental data and the model predictions. As explained in Adams and Gelhar (1992) and Salamon et al. (2007), the displayed data were obtained by interpolation of concentration values between sampling wells, vertical and transverse integration of the resulting concentration field, and longitudinal averaging over a window of $\Delta x = 10$ m (Adams & Gelhar, 1992; Salamon et al., 2007). The bin centers are located at $x_i = -15\ \text{m} + i10\ \text{m}$ with $i = 0, ..., 19$. The injection position is at $x = 0$. Concentration values are normalized by the initial mass. The longitudinal concentration distribution is shown at six snapshots at times $t = 49$, 126, 202, 279, 370, and 503 days for MADE-1 and at $t = 27$ and 328 days for MADE-2. The tracer distributions predicted from the upscaled model are presented in the same way. Section S4 provides the tracer distributions with an averaging window of $\Delta x = 10^{-1}$ m for MADE-1. We refer to the latter as the fine-scale model data.

We first note that the experimental data do not integrate to 1. In fact, the mass under the longitudinal profiles for the MADE-1 data integrates to 2.06, 0.99, 0.68, 0.62, 0.54, and 0.43 for the six snapshots at increasing time (Adams & Gelhar, 1992; Fiori et al., 2013) and to 1.52 and 0.77 at $t = 27$ and 328 days for the MADE-2 snapshots (Stauffer et al., 1994). The explanation of this apparent mass loss has been a matter of debate in the literature. Several authors (Boggs & Adams, 1992; Harvey & Gorelick, 2000; Molz et al., 2006; Salamon et al., 2007) attribute the overestimation of mass at early and underestimation at late times to a measurement bias due to preferential sampling from high conductivity regions and mass transfer into immobile regions. In fact, the analysis of core samples 2 years after the MADE-1 experiment by Boggs and Adams (1992) indicate that a substantial amount of mass may have been transferred and stored in immobile zones. Other authors (Adams & Gelhar, 1992; Fiori et al., 2013) debate that the mass loss could be attributed to a decreasing density of sampling points at distances larger than 20 m downstream from the injection region. This view is supported by the fact that more mass loss is observed for the bromide plume in the MADE-1 (Adams & Gelhar, 1992) than for the tritium plume in the MADE-2 experiment (Stauffer et al., 1994), for which the density of sampling wells was increased.

The tracer distribution in the upscaled TDRW model is by default normalized to $1/\theta$, which, as outlined above, accounts for a possible sampling bias due to adsorption. Figures 2 and 3 display model predictions for $K_g = 5.5 \times 10^{-6}$ m/s, $K_g = 10^5$ m/s, and $K_g = 4.3 \times 10^{-6}$ m/s at the upper and lower limits of the confidence interval. The model predicts the overall shape of the observed tracer distributions, the slow moving peak, and the development of a forward tail with increasing time. For increasing K_g, the velocity spectrum is shifted to higher values. Thus, the peak height and peak retention decrease and the forward tail increases. While the value of $K_g = 5.5 \times 10^{-6}$ m/s provides the best prediction for the peak concentrations, all K_g values give qualitatively the same non-Gaussian tracer profiles. This shows the robustness of the salient

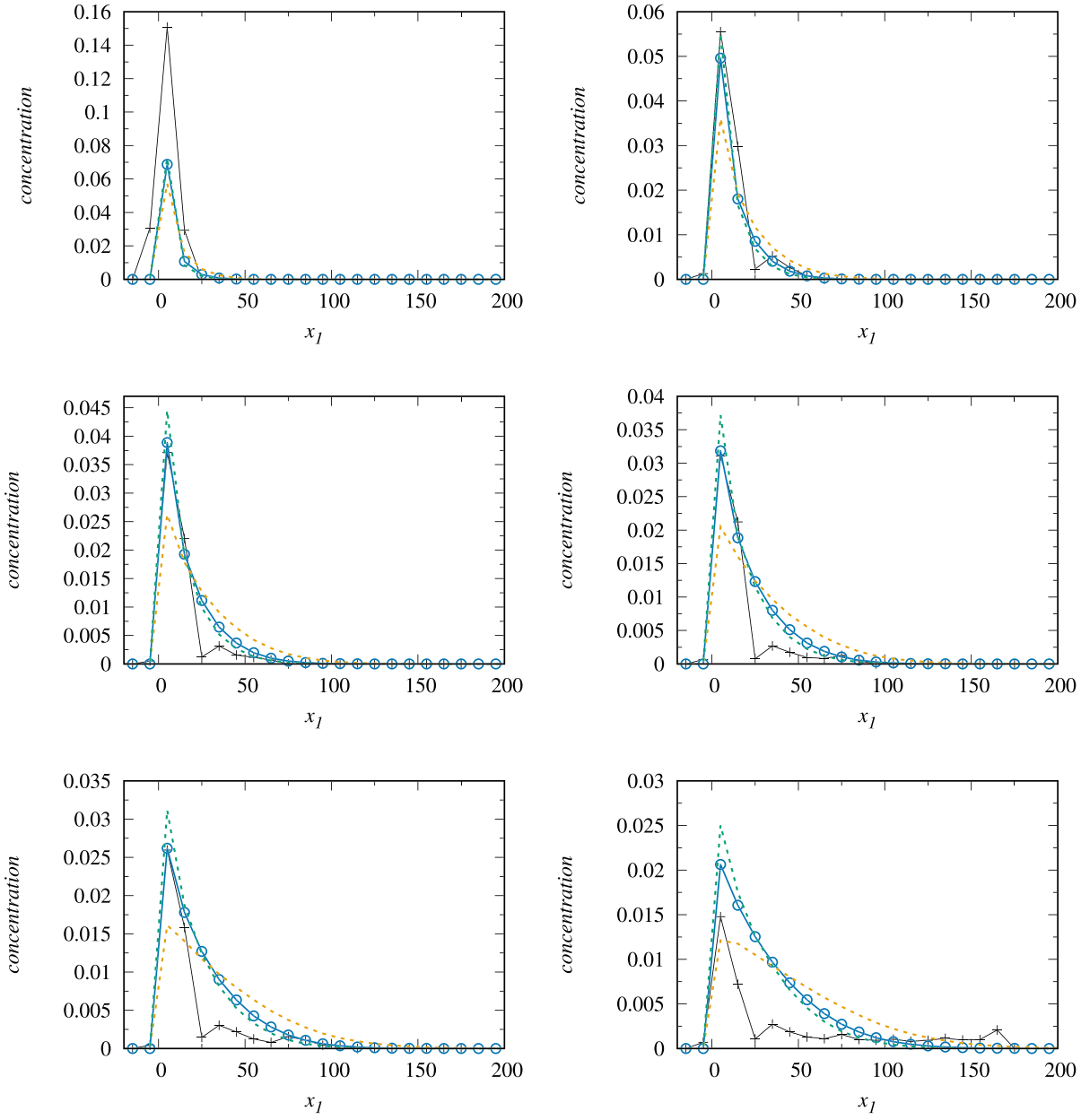

Figure 2. Concentration profiles from (crosses) the MADE-1 data and (circles) the upscaled model for an averaging window of $\Delta x = 10$ m at times (top left to bottom right) $t = 49$, 126, 202, 279, 370, and 503 days using a pointlike initial distribution. The dashed lines denote the predictions for the values of (green) $K_g = 4.3 \times 10^{-6}$ m/s and (orange) $K_g = 10^5$ m/s at the lower and upper limits of the 95% confidence interval of K_g.

non-Gaussian transport features predicted by the TDRW approach. The upscaled model accounts for retention of tracer mass in the injection region through persistent low initial flow speeds. The forward tailing is accounted for through the presence of high initial flow velocities in combination with fast tracer motion through particle transitions into spatially persistent fast velocity channels.

The predicted mass in the tails at 126 to 370 days (MADE-1) is generally higher for $x > 25$ m than in the experimental data, while the reach is relatively well reproduced; see also the corresponding logarithmic plots in section S4. As mentioned above, this discrepancy between model and data may be attributed to a decreasing density of sampling points more than 20 m downstream from the injection (Adams & Gelhar, 1992; Fiori et al., 2013). The last snapshots at $t = 503$ days for the MADE-1 and $t = 328$ days for the MADE-2

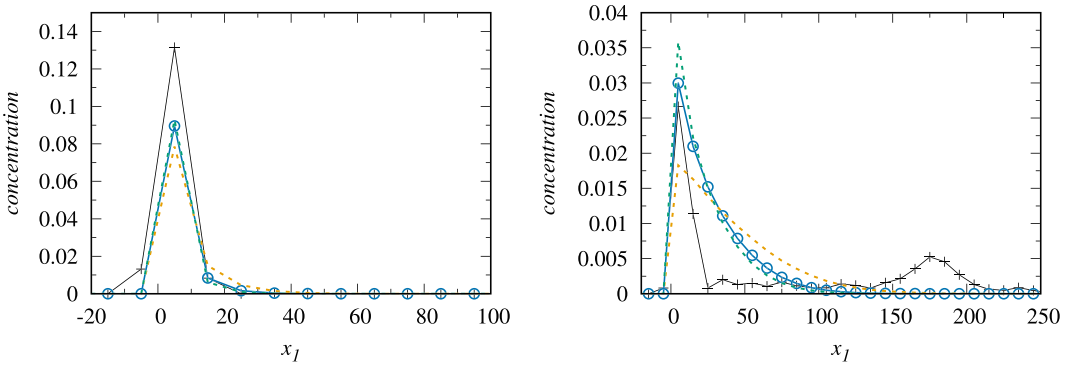

Figure 3. Analogous to Figure 2 for the concentration profiles of the MADE-2 experiments at $t = 27$ and 328 days.

experiments show farther reaching forward tails with secondary peaks, which are not captured by the TDRW model. These features in the data may be attributed to a sampling bias.

4. Conclusions

We have presented a Lagrangian stochastic model for transport in heterogeneous aquifers that is parameterized in terms of the statistical characteristics of hydraulic conductivity and Eulerian flow speed. The approach is based on a Markov processes for equidistant particle speed, whose steady-state distribution is given by the flux-weighted flow speed distribution. The latter is derived from the distribution of the Eulerian flow speed, which is obtained from standardized numerical flow simulations, meaning for unit gradient of hydraulic head and unit geometric mean conductivity. The model is parameterized by the mean, variance, and correlation lengths of the logarithm of hydraulic conductivity, advective tortuosity, and porosity. These model inputs are transport-independent, that is, they can be assessed by medium and flow characterization. These features yield a predictive upscaled approach for advective tracer transport in heterogeneous aquifers. Like other stochastic models, this approach relies on the ergodicity of the underlying medium heterogeneity. The model furthermore accounts for linear instantaneous equilibrium sorption.

We use this upscaled model to assess and predict the evolution of the bromide tracer plume of the MADE-1 and the tritium plume of the MADE-2 experiments, which are characterized by strongly non-Gaussian shapes. Relatively low conductivity in the source zone leads to slow peak movement of only a few meters over the duration of the experiments, while part of the tracer moves fast, which gives rise to a pronounced forward tail. The slow moving peak is captured by the upscaled model through the low velocity end in the distribution of initial particle speeds. The developing forward tail is quantified by tracer propagation due to spatially persistent broadly distributed particle speeds. The speed distributions are determined by the medium and Eulerian flow statistics. As mentioned above, all model parameters are obtained from transport-independent measurements without recourse to fitting parameters. We find that the purely advective upscaled model provides a robust estimate of the evolution of the overall plume shape. Our results indicate that the large-scale transport features of the MADE-1 and MADE-2 plumes may be explained by flow heterogeneity due to spatial variability in hydraulic conductivity. The proposed upscaled model is predictive, transferable to different solutes and hydraulic conditions, and seems to capture the salient heterogeneity mechanisms and their impact on large-scale transport.

Data Availability Statement

The experimental data were published originally in Adams and Gelhar (1992) and reproduced in Fiori et al. (2013), from where the data in the present work is obtained. The TDRW model data are available at https://doi.org/10.20350/digitalCSIC/12667.

Acknowledgments

We thank Daniel Fernandez-Garcia for sharing the data for the two concentration snapshots of the MADE-2 experiment and Alraune Zech and Aldo Fiori for sharing the MADE-1 data with us. The authors acknowledge the financial support of the European Research Council through the project MHetScale (Grant Agreement No. 617511) and the Spanish Ministry of Science and Innovation through a Severo Ochoa project (No. CEX2018-000794-S) and the project HydroPore (PID2019-106887GB-C31). Juan J. Hidalgo acknowledges the support of the Spanish Ministry of Science and Innovation through a Ramón y Cajal fellowship (No. RYC-2017-22300). Alessandro Comolli acknowledges support through the Prodex grant CHYPI.

References

Adams, E. E., & Gelhar, L. W. (1992). Field study of dispersion in a heterogeneous aquifer: 2. Spatial moment analysis. *Water Resources Research*, *28*, 3293–3307.

Barlebo, H. C., Hill, M. C., & Rosbjerg, D. (2004). Investigating the Macrodispersion Experiment (MADE) site in Columbus, Mississippi, using a three-dimensional inverse flow and transport model. *Water Resources Research*, *40*, W04211. https://doi.org/10.1029/2002WR001935

Bear, J. (1972). *Dynamics of fluids in porous media*. New York: American Elsevier.

Benson, D. A., Schumer, R., Meerschaert, M. M., & Wheatcraft, S. W. (2001). Fractional dispersion, Lévy motion, and the MADE tracer tests. *Transport in Porous Media*, *42*(1–2), 211–240.

Benson, D. A., Wheatcraft, S. W., & Meerschaert, M. M. (2000). Application of a fractional advection-dispersion equation. *Water Resources Research*, *36*(6), 1403–1412.

Berkowitz, B., Cortis, A., Dentz, M., & Scher, H. (2006). Modeling non-Fickian transport in geological formations as a continuous time random walk. *Reviews of Geophysics*, *44*, RG2003.

Berkowitz, B., & Scher, H. (1997). Anomalous transport in random fracture networks. *Physical Review Letters*, *79*(20), 4038–4041.

Berkowitz, B., & Scher, H. (1998). Theory of anomalous chemical transport in fracture networks. *Physical Review E*, *57*(5), 5858–5869.

Boggs, J. M., & Adams, E. E. (1992). Field study of dispersion in a heterogeneous aquifer: 4. Investigation of adsorption and sampling bias. *Water Resources Research*, *28*(12), 3325–3336. https://doi.org/10.1029/92wr01759

Boggs, J., Beard, L., Waldrop, W., Stauffer, T., MacIntyre, W., & Antworth, C. (1993). Transport of tritium and four organic compounds during a natural-gradient experiment (MADE-2) (*Tech. Rep.*): Electric Power Research Inst., Palo Alto, CA (United States); Tennessee Valley Authority, Norris, TN (United States). Engineering Lab.; Air Force Engineering and Services Center, Tyndall AFB, FL (United States.

Boggs, J. M., Young, S. C., Beard, L. M., Gelhar, L. W., Rehfeldt, K. R., & Adams, E. E. (1992). Field study of dispersion in a heterogeneous aquifer: 1. Overview and site description. *Water Resources Research*, *28*, 3281–3291.

Bohling, G. C., Liu, G., Dietrich, P., & Butler, J. J. (2016). Reassessing the MADE direct-push hydraulic conductivity data using a revised calibration procedure. *Water Resources Research*, *52*, 8970–8985. https://doi.org/10.1002/2016wr019008

Carrera, J., Sánchez-Vila, X., Benet, I., Medina, A., Galarza, G., & Guimerà, J. (1998). On matrix diffusion: Formulations, solution methods, and qualitative effects. *Hydrogeology Journal*, *6*, 178–190.

Comolli, A., Hakoun, V., & Dentz, M. (2019). Mechanisms, upscaling, and prediction of anomalous dispersion in heterogeneous porous media. *Water Resources Research*, *55*, 8197–8222. https://doi.org/10.1029/2019wr024919

Cushman, J., & Ginn, T. (1993). Non-local dispersion in media with continuously evolving scales. *Transport in Porous Media*, *13*(1), 123–138.

Cushman, J. H., & Ginn, T. R. (2000). Fractional advection-dispersion equation: A classical mass balance with convolution-Fickian flux. *Water Resources Research*, *36*, 3763–3766.

Cvetkovic, V., Cheng, H., & Wen, X.-H. (1996). Analysis of nonlinear effects on tracer migration in heterogeneous aquifers using Lagrangian travel time statistics. *Water Resources Research*, *32*(6), 1671–1680.

Cvetkovic, V., Fiori, A., & Dagan, G. (2014). Solute transport in aquifers of arbitrary variability: A time-domain random walk formulation. *Water Resources Research*, *50*, 5759–5773. https://doi.org/10.1002/2014WR015449

Dagan, G. (1984). Solute transport in heterogenous porous formations. *Journal of Fluid Mechanics*, *145*, 151–177.

Dagan, G. (1989). *Flow and transport in porous formations*. New York: Springer.

de Anna, P., Le Borgne, T., Dentz, M., Tartakovsky, A. M., Bolster, D., & Davy, P. (2013). Flow intermittency, dispersion and correlated continuous time random walks in porous media. *Physical Review Letters*, *110*(184), 502.

Dentz, M., Kang, P. K., Comolli, A., Le Borgne, T., & Lester, D. R. (2016). Continuous time random walks for the evolution of Lagrangian velocities. *Physical Review Fluids*, *1*(7), 074004.

Dentz, M., Le Borgne, T., Englert, A., & Bijeljic, B. (2011). Mixing, spreading and reaction in heterogeneous media: A brief review. *Journal of Contaminant Hydrology*, *120–121*, 1–17.

Dogan, M., Van Dam, R. L., Liu, G., Meerschaert, M. M., Butler, Jr. J. J., Bohling, G. C., et al. (2016). Predicting flow and transport in highly heterogeneous alluvial aquifers. *Geophysical Research Letters*, *41*, 7560–7565. https://doi.org/10.1002/2014GL061800

Doob, J. L. (1942). The Brownian movement and stochastic equations. *Annals of Mathematics*, *43*, 351–369.

Edery, Y., Guadagnini, A., Scher, H., & Berkowitz, B. (2014). Origins of anomalous transport in heterogeneous media: Structural and dynamic control. *Water Resources Research*, *50*, 1490–1505.

Feehley, C. E., Zheng, C., & Molz, F. J. (2000). A dual-domain mass transfer approach for modeling solute transport in heterogeneous aquifers: Application to the Macrodispersion Experiment (MADE) site. *Water Resources Research*, *36*(9), 2501–2515. https://doi.org/10.1029/2000wr900148

Fiori, A., Dagan, G., Jankovic, I., & Zarlenga, A. (2013). The plume spreading in the MADE transport experiment: Could it be predicted by stochastic models? *Water Resources Research*, *49*, 2497–2507. https://doi.org/10.1002/wrcr.20128

Fiori, A., Jankovic, I., Dagan, G., & Cvetkovic, V. (2007). Ergodic transport through aquifers of non-Gaussian log conductivity distribution and occurrence of anomalous behavior. *Water Resources Research*, *43*, W09407. https://doi.org/10.1029/2007WR005976

Gardiner, C. W. (1986). Handbook of stochastic methods for physics, chemistry and the natural sciences. *Applied Optics*, *25*, 3145.

Gelhar, L. W. (1993). *Stochastic subsurface hydrology*. Englewood Cliffs, NJ: Prentice Hall.

Gelhar, L. W., & Axness, C. L. (1983). Three-dimensional stochastic analysis of macrodispersion in aquifers. *Water Resources Research*, *19*(1), 161–180.

Guan, J., Molz, F. J., Zhou, Q., Liu, H. H., & Zheng, C. (2008). Behavior of the mass transfer coefficient during the MADE-2 experiment: New insights. *Water Resources Research*, *44*, W02423. https://doi.org/10.1029/2007wr006120

Haggerty, R., & Gorelick, S. M. (1995). Multiple-rate mass transfer for modeling diffusion and surface reactions in media with pore-scale heterogeneity. *Water Resources Research*, *31*(10), 2383–2400.

Haggerty, R., McKenna, S. A., & Meigs, L. C. (2000). On the late time behavior of tracer test breakthrough curves. *Water Resources Research*, *36*(12), 3467–3479.

Hakoun, V., Comolli, A., & Dentz, M. (2019). Upscaling and prediction of Lagrangian velocity dynamics in heterogeneous porous media. *Water Resources Research*, *55*, 3976–3996. https://doi.org/10.1029/2018WR023

Harvey, C., & Gorelick, S. M. (2000). Rate-limited mass transfer or macrodispersion: Which dominates plume evolution at the Macrodispersion Experiment (MADE) site? *Water Resources Research*, *36*(3), 637–650.

Hyman, J. D., Dentz, M., Hagberg, A., & Kang, P. K. (2019). Linking structural and transport properties in three-dimensional fracture networks. *Journal of Geophysical Research: Solid Earth*, *124*, 1185–1204. https://doi.org/10.1029/2018jb016553

Kang, P. K., de Anna, P., Nunes, J., Bijeljic, B., Blunt, M. J., & Juanes, R. (2014). Pore-scale intermittent velocity structure underpinning anomalous transport through 3-D porous media. *Geophysical Research Letters*, *41*, 6184–6190. https://doi.org/10.1002/2014GL061475

Kang, P. K., Dentz, M., Le Borgne, T., & Juanes, R. (2011). Spatial Markov model of anomalous transport through random lattice networks. *Physical Review Letters*, *107*(180), 602.

Kang, P. K., Dentz, M., Le Borgne, T., Lee, S., & Juanes, R. (2017). Anomalous transport in disordered fracture networks: Spatial markov model for dispersion with variable injection modes. *Advances in Water Resources*, *106*, 80–94. https://doi.org/10.1016/j.advwatres.2017.03.024

Kang, P. K., Le Borgne, T., Dentz, M., Bour, O., & Juanes, R. (2015). Impact of velocity correlation and distribution on transport in fractured media: Field evidence and theoretical model. *Water Resources Research*, *51*, 940–959. https://doi.org/10.1002/2014WR015799

Le Borgne, T., Dentz, M., & Carrera, J. (2008). Spatial Markov processes for modeling Lagrangian particle dynamics in heterogeneous porous media. *Physical Review E*, *78*(041), 110.

Levy, M., & Berkowitz, B. (2003). Measurement and analysis of non-Fickian dispersion in heterogeneous porous media. *Journal of Contaminant Hydrology*, *64*(3–4), 203–226.

Molz, F. J., Zheng, C., Gorelick, S. M., & Harvey, C. F. (2006). Comment on "Investigating the Macrodispersion Experiment (MADE) site in Columbus, Mississippi, using a three-dimensional inverse flow and transport model" by Heidi Christiansen Barlebo, Mary C. Hill, and Dan Rosbjerg. *Water Resources Research*, *42*, W06603. https://doi.org/10.1029/2005wr004265

Morales, V. L., Dentz, M., Willmann, M., & Holzner, M. (2017). Stochastic dynamics of intermittent pore-scale particle motion in three-dimensional porous media: Experiments and theory. *Geophysical Research Letters*, *44*, 9361–9371. https://doi.org/10.1002/2017GL074326

Neuman, S. P. (1993). Eulerian-Lagrangian theory of transport in space-time nonstationary velocity fields: Exact nonlocal formalism by conditional moments and weak approximation. *Water Resources Research*, *29*(3), 633–645.

Neuman, S. P., & Tartakovsky, D. M. (2008). Perspective on theories of anomalous transport in heterogeneous media. *Advances in Water Resources*, *32*, 670–680. https://doi.org/10.1016/j.advwatres.2008.08.005

Noetinger, B., Roubinet, D., Russian, A., Le Borgne, T., Delay, F., Dentz, M., et al. (2016). Random walk methods for modeling hydrodynamic transport in porous and fractured media from pore to reservoir scale. *Transport in Porous Media*, *115*, 345–385.

Puyguiraud, A., Gouze, P., & Dentz, M. (2019a). Upscaling of anomalous pore-scale dispersion. *Transport in Porous Media*, *128*(2), 837–855. https://doi.org/10.1007/s11242-019-01273-3

Puyguiraud, A., Gouze, P., & Dentz, M. (2019b). Stochastic dynamics of Lagrangian pore-scale velocities in three-dimensional porous media. *Water Resources Research*, *55*, 1196–1217. https://doi.org/10.1029/2018wr023702

Rubin, Y. (2003). *Applied stochastic hydrogeology*. New York: Oxford University Press.

Salamon, P., Fernàndez-Garcia, D., & Gómez-Hernández, J. J. (2007). Modeling tracer transport at the made site: The importance of heterogeneity. *Water Resources Research*, *43*, W08404. https://doi.org/10.1029/2006WR005522

Schumer, R., Benson, D. A., Meerschaert, M. M., & Bauemer, B. (2003). Fractal mobile/immobile solute transport. *Water Resources Research*, *39*(10), 1296. https://doi.org/10.1029/2003WR002141

Stauffer, T. B., Antworth, C. P., Young, R. G., MacIntyre, W. G., & Boggs, J. (1994). Degradation of aromatic hydrocarbons in an aquifer during a field experiment demonstrating the feasibility of remediation by natural attenuation (*Tech. rep.*): Tennessee Valley Authority Norris.

Tyukhova, A., Dentz, M., Kinzelbach, W., & Willmann, M. (2016). Mechanisms of anomalous dispersion in flow through heterogeneous porous media. *Physical Review Fluids*, *1*(7), 074002.

Zhang, Y., & Benson, D. A. (2008). Lagrangian simulation of multidimensional anomalous transport at the MADE site. *Geophysical Research Letters*, *35*, L07403. https://doi.org/10.1029/2008gl033222

Zheng, C., Bianchi, M., & Gorelick, S. M. (2011). Lessons learned from 25 years of research at the MADE site site. *Groundwater*, *49*(5), 649–662.